Hindawi
Security and Communication Networks
Volume 2022, Article ID 6424835, 18 pages
https://doi.org/10.1155/2022/6424835

*Research Article*

# Accident Detection in Autonomous Vehicles Using Modified Restricted Boltzmann Machine

**Roohullah**,[1] **Fazli Wahid**,[1] **Sikandar Ali**,[1] **Irshad Ahmed Abbasi**,[2] **Samad Baseer**,[3] **and Habib Ullah Khan**[4]

[1]*Department of Information Technology, The University of Haripur, Haripur 22620, Khyber Pakhtunkhwa, Pakistan*
[2]*Department of Computer Science, Faculty of Science and Arts Belqarn, University of Bisha, Sabt Al-Alaya 61985, Saudi Arabia*
[3]*Department of Computer System Engineering, University of Engineering and Technology, Peshawar 25000, Pakistan*
[4]*Department of Accounting and Information Systems, College of Business and Economics, Qatar University, Doha 2713, Qatar*

Correspondence should be addressed to Fazli Wahid; fazli.wahid@uoh.edu.pk, Sikandar Ali; sikandar@uoh.edu.pk, and Habib Ullah Khan; habib.khan@qu.edu.qa

Received 22 January 2022; Revised 21 April 2022; Accepted 23 April 2022; Published 30 June 2022

Academic Editor: Muhammad Shafiq



Accident detection in autonomous vehicles could save lives by reducing the time it takes for information to reach emergency responder. One of the most common reason for the death of humans is accident. Indeed, it was determined throughout the survey that road accidents are indeed the second greatest cause of death in the United States for people aged 30 to 44 years, representing for 1/3 among all deaths. The transportation industry is increasingly relying on mathematical methods and new data assets to detect injuries. Many machine learning and deep learning models have already been proposed for accident detection but still there is much space for further improvement to be done to save human lives in case of accident detection, if accidents are not identified well. In our present study, we proposed modified restricted Boltzmann machine for accident detection. Our proposed methodology consists of the following steps. In the first step, we took different accidental and nonaccidental images as an input. In the second step, we applied our proposed deep learning technique modified restricted Boltzmann machine. In the third step, when weight acceleration and coefficient adjustments are run as a generalization mechanism, then we check our model performance after applying through multiple procedures. As a result, multiple images are classified as accidental and nonaccidental images of vehicles. Proposed methodology has been applied for data set, and data have been divided into different training and testing ratios. The proposed MRBM model has an accuracy of 98% in classification of both accidental and nonaccidental images of vehicles. The proposed model outperforms the competition significantly than other in which they are compared like artificial neural network, support vector machine, and restricted Boltzmann machine techniques.

## 1. Introduction

Accidents in the international-huge are one of the most severe challenges. Every day, as the number of roadways and automobiles grows, so does the amount of injuries suffer in the business. About 5 million people deaths are involved in crashes in the United States each year according to National Highway Traffic Safety Administration. Indeed, it was determined throughout the survey that road accidents are indeed the second greatest cause of death in the United States for people aged 30 to 44 years, representing for 1/3 among all deaths. Injury-causing road accidents increased by 3% to 2% during 2011 and 2012 [1]. According to the World Health Organization, 1.25 million people die each year as a result of accidents occurred at crossing points. Aside from the impact on human fitness, visitor accidents have a detrimental influence on crossing points, particularly highways, intersection factors, and work places. If accidents are not identified well and soon lots of lives will be lost every year. The transportation industry is increasingly relying on mathematical methods and new data assets to detect injuries. Vision-based whole-accident detection, on the other hand, demands a large amount of data supplied by images and movies and a lot of storage. In actuality, because social media

data are less freely available than traffic records, it is more than a major source of information for accident detection. Car crashes are the top cause of death in the United States. Automatic car crash detection could save lives by lowering the time required for data to reach emergency personnel. Vehicular sensor systems for obstacle detection, including such OnStar, use in-car detectors to detect vehicle injuries and incorporated cell phones to contact emergency services instantly. Wi-Fi cell monitoring systems are increasingly being used for car collision identification and toll way congestion control. Smartphone advances have made it possible to detect car crashes in a more transportable and cost-effective manner as compared in-vehicle solutions. Existing traffic data are a large and generally available source of data that can be used to detect collisions. The majority of highways and freeways in the United States have loop detector data. Using traffic data to detect accidents, a variety of strategies have been explored. In addition, numerous gadget examining trends, such as k-nearest neighbour, regression tree, feed-forward neural network, assist vector machine, and probabilistic neural network, have been employed to find injuries. We will use machine learning techniques to deduce the elegance of the most recent pattern from previously labelled samples. We can utilise supervised learning of a term for a category because supervised learning of a set of rules is provided with a training pattern and its matching output. Each consequence or result exemplifies the pattern's brilliance. This research employs machine learning techniques.

Artificial neural networks (ANNs) are used to modify the behaviour of a real neural network made up of many linked neurons. ANN is a network of nodes that transforms a weight value of inputs into a "0" or "1" output value. In each node, a sigmoidal transferring function converts the weighted total to the output. The neural community's input nodes are as many as the inputs themselves, and the output has a diverse set of outputs that are discussed by a diverse set of classes. Only one output is necessary whether there are two classes. An ANN with numerous layers is known as a multilayer perceptron. Nodes of the hidden layer are connected directly to input neurons, and network output is connected to a single output node. One of the input neurons has a direct link to the output node, in addition to these connections. Each node-to-node connection in ANN is assigned a weight. The on-board unit (OBU) standard is critical for the proposed device. Because it could be used in a broad range of vehicles in the near future, this device must be cost effective. This system also needs to be able to receive updates to the destiny software. Although the arrangement of the equipment to be handled in cars initially consisted of special-motive systems, this tendency is getting closer to existing schemes due to the constant inclusion of new products. Information is exchanged between the OBUs and the CU via the Internet, through either vehicles that give Internet connection (such as UMTS) or by fixed network devices (roadside units, RSU). If the car does not have immediate access to the CU, this could produce messages that are broadcast to other cars until they hit one of the communication pathways listed above. These communications, in addition to advising vehicles travelling through the accident site about the state of the impacted car and its possible influence on regular traffic flow [2], are also transmitted to several cars within the accident location. IDIADA's crash tests acquire a huge quantity of data on the accident (10,000 samples per 2d) that cannot be processed in actual, thus it must be evaluated after the event off-line. However, vital machine data should be obtained in the second strange twist in limiting the time to relax and the consequences of the crash on the passengers.

According to a recent study report released by the NHTSA (National Highway Traffic Safety Administration), 94% of all traffic accidents are caused solely by human error. Due to factors such as lack of attention while driving, fog weather, reflections of lights, and anonymous objects, the driver may be unable to adequately recognise items from his position in various situations [3]. It results in tragic accidents in certain scenarios [1]. To address the aforementioned issues, autonomous vehicles (AV) were developed, which employ the advanced driving assistance system (ADAS). This technology takes into account the surrounding environment and offers solutions for improving road safety, reducing traffic, reducing emissions, and improving passenger comfort. Autonomous components are made composed of many sensors that are utilised to keep track of the surroundings while driving [2]. In comparison to vehicles driven by humans, these vehicles reduce human labour during driving and enhance driving safety [4, 5]. For accident detection, we suggested the modified restricted Boltzmann machine in this paper. The steps in our proposed methodology are as follows. As a starting point, we used a variety of inadvertent and nonaccidental photographs as input. In the second stage, we used the modified restricted Boltzmann machine, a deep learning technique we invented. We examine our model performance after applying several processes in the third stage, where weight acceleration and coefficient modifications are run as a generalization mechanism. As a result, several photos of automobiles are classed as accidental and nonaccidental. The proposed methodology was used on the data set, and the data were separated into various training and testing ratios. The suggested MRBM model has a classification accuracy of 98% for both accidental and nonaccidental vehicle photos. Accidental and nonaccidental vehicles are categorized here in Figures 1–4.

These are some images of accidental (Figures 1 and 2) [6] and non-accidental (Figures 3 and 4) [7] cars on road.

## 2. Literature Work

Many machine learning methods and algorithms have been used in the past to detect accidents in autonomous vehicles. This section discusses some of the past works that has been completed recently. Problem checking out, modelling multimodal trajectories, multimodal optimization function, and lane-following multimodal prediction are some of the steps taken by the researcher Cui et al. [6]. Also, the effect reveals that we set a five-point threshold for the attitude difference. Then, any modes that diverge by less than five

Figure 1: Hyundai car on road.

Figure 2: Audi car on road.

Figure 3: Collision of vehicle.

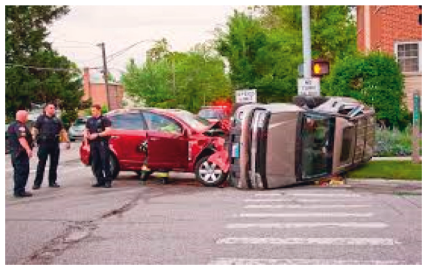

Figure 4: Crash between two cars.

from the floor-reality trajectory. We can see that basic optimization allows the model to generalise effectively in both intersection and straight-road cases. Sensing layer, networking layer, utility layer, and deep learning approaches are some of the strategies that researcher Chang [7] can employ. The deep crash system consists of an IVI telecommunication infrastructure with car collision sensor devices, an Internet deep learning server, and an Internet comprehensive management platform. Typically, Internet statistics platforms transmit alert message and alerts based on the accident prediction outcome, and traffic coincidence GPS functionality is available. These are among the methods that the investigator might employ in this investigation. The terms "logistic regression," "random forest," "support vector machine," and "comparison parameters" are used interchangeably. Dogru and Subasi [8]. This implies that automobile incidents in the United States continue to be a safety concern for kingdom road groups around the country. Large areas have a complicated road network, with high speeds, various entry sites, and constant traffic weaving. Vehicle kinematic and dynamic data, physiological sensor data, sight records, eye-data, ground, physiological statistics, and all modalities were used by researcher Misra [9]. This study was conducted with young drivers, and the results show their reaction to dangerous driving in comparison to regular driving with no secondary challenge. Li [10] employed generative adverse community, temporal and spatial stacked car encoder (TSSAE), and the built hybrid model as techniques. Actual and produced incident samples, GAN effectiveness, and TSSAE effectiveness were all evaluated. Ignoring the fact that the suggested hybrid model can accurately and successfully identify visitor incidents, future study could make a few enhancements. For the identification and categorization of pictures, a number of methodologies have been presented, with deep mastering approaches being one of the most recent [3, 11].

The use of a generative adversarial network (GAN) is used to address the issue of small pattern length and imbalance in site visitor incident data sets. Guidelines for choosing temporal and spatial variables are offered, which might be effective in capturing the spatial and temporal patterns of visitor flow. Some of the strategies used by scholar Tumen [12] include databases and data, preprocessing for data sets, and a proposed CNN model. Using a transferring car, we identified crucial toll road portions such as street junctions, road separations, and crosswalks. Moreover, efficiency quotes were compared across several CNN network architectures, including such Alex Net, LeNet, and VggNet, all which provided positive results in numerous studies using the RoIC-CNN versions, and the findings of our variant were contrasted to similar studies in the literature. Tieleman et al. developed the rapid chronic contrastive divergence method as a solution to improve the PCD algorithm. Extra rapid parameters were introduced in 2009 [13] to improve sampling speed. The paralleled temper set of rules (PT) based on sample era was proposed by Parsa et al. [14] and Larochelle et al. [15] in 2010. In multimode goal distribution, the PT algorithm was developed to overcome the limitations of traditional sampling algorithms. Experiments show that the PT guideline can produce superior techniques for RBM training while also effectively preventing any possible divergence. There are several articles that use deep learning techniques in the prediction of traffic flow. One of the maximum exciting article is the thing through MA 2017 [7]. This article describes an approach to assess traffic flow as photos. These pictures should then be used to expect the following kingdom of the community the use of a convolutional neural community (CNN). The article of Bratsas 2019 [4] preformed an assessment on different machine studying methods for traffic pace prediction. In his article, Bratsas states that the multilayer perceptron model (MLP) works

satisfactory for occasions with awesome versions. Because a CNN works quicker and is more accurate than an MLP, this research focuses on the use of a CNN, with using images to symbolize the network through the years. Next to these articles where identified close to collision detection [1, 2, 8], these articles take equal approach as this studies in the direction of predicting speed and course of specific motors. The performance of camera-based method as developed by Chung [8] completely indicates driver sleepiness, but its implementation is limited due to its huge expenses. Methods used by researcher Jae-joon Chung [8] are air quality sensor (AQS), IOT sensor platform, deep learning-based sensors, and deep learning-based anomaly detection. We additionally analysed the development traits of generation for facilitating DSD within the context of ADASs. Sleepiness prevention devices have been developed in a number of fields. It was found that their adoption is confined through problems consisting of high price and occasional detection accuracy. We used a low-price sensor with simple specifications, included it with a deep learning model, and proved its greater effectiveness in detecting abnormalities in the interior surroundings of a vehicle, as compared to existing strategies. To provide site visitor data, 1st Baron Verulam et al. [9] used actual traffic data from fixed and stuck sensors to assess the degree of tourist congestion in the city. [3].

Support vector machine was used to adapt a motorway incident detection method for the current situation in the city. Li et al. [10] developed a system capable of detecting visitor's incidents and traffic jams in real time by combining the rate of motor vehicles travelling the road segment with a set of threshold values. Methods used by researcher are validating the unmodified reference system and evaluation towards the recreation of the May seventh Tesla accident in Florida. It was inspired by means of numerous crucial early accidents concerning SAE Level II self-sustaining automobiles that highlighted sudden safety hazards in their design that have been justified by using an over-reliance on operator oversight that turned into not properly implemented or enforced. In order to assist prevent future accidents. In a few states of affairs, the driver cannot be capable of become aware of the items from his function nicely due to the subsequent reasons like lack of interest at the same time as driving, because of fog weather, mirrored image of the lighting and nameless gadgets etc. In those situations, it leads to the fatal injuries [2]. Methods used by researcher Misra [9] are Object detection, deep reinforcement, YOLO, GPS, Lidar, Radar, Convolutional neural community, deep gaining knowledge of and gadget gaining knowledge of strategies are used. Autonomous Vehicle is driverless vehicle which contains improve using assistant device to understand the environment through sensors. The important goal of AV is driving the vehicle with nonhuman involvement. To obtain this AV's entails the distinctive sensors like LIDAR, RADAR, CAMERA, GPS and Ultrasonic Sensor. The data from these sensors is analysed using cutting-edge device learning and deep learning object detection algorithms such as SVM, CNN, Fast R–CNN, Faster R–CNN, and YOLO. Researchers were able to create computerised accident detection systems thanks to recent advances in synthetic intelligence technology. The status of site visitor flow might be classified as ordinary or accidental in these investigations. Time collecting, pattern popularity tactics, fuzzy set filtering, and help vector system are some of the other strategies (SVM). Using SVM, several coincidence detection algorithms were created and tested on actual limited-access highway data. For the same data set, SVM-based strategies outperformed neural community-based techniques in terms of overall performance in detecting injuries [16].

ECall [10]: the eCall device was designed to improve transport safety by providing emergency support to anyone in the event of a crash anywhere else in the Euro Zone. An urgent voice call is initiated in the event of an accident, and it is sent through the mobile phone network to emergency services. ECall also transmits a minimum set of data (MSD) that includes critical accident information and time, position, and car description. It is anticipated that the eCall gadget will be operational by 2015. Chen et al. [16] measured the crossing signs on the road at different times of the day. Before categorising the photographs in the database, he binary filtered all 50 of them. During this inquiry, it became evident that no meaningful preprocessing had taken place. During the examination, it was discovered that there was no major preprocessing, and the low-cost images were classified with a success rate of 92%. Deep studying methodologies and artificial neural strategies have been used in recent research on highway, lane commitment, object recognition, pedestrian and traffic signals, and symptoms on roads [11–14, 3035]. In the willpower of traffic intersections, the laser imaging detection and ranging (LiDAR) signalling device has been used [12, 35, and 36]. However, this detection device outperforms the others in terms of speed. When looking at the outcomes of a study into the material about street kinds, it is evident that the emphasis has changed to identifying junctions, separations, and crossings. Steps used are preprocessing layer, feature extraction, and object detection layer. The next input is tracking MTMV using CKFA and MVTA, which has a 95.5% accuracy compared to the current method. The steps that were completed were data acquisition, image analysis, modelling, and model development. It is the first time a CNN is used to ask many questions of texting while driving, according to the study, with fantastic results as well as the designed to perceive the reckless driver with high sensitivity. The accuracy achieved by CNN is as continues to follow: the blue line represents the teaching facts activity, with a production of quality products of 0.93, whereas the orange line represents the testing data performance, with a production of quality products of 0.95. Amir Bahador Parsaa [17] used approaches such as synthetic minority oversampling technique (SMOTE), support vector machine (SVM), probabilistic neural network (PNN), and model validation.

To categorise the massive amount of 3D data acquired from the sensors, the author proposed a semisupervised machine learning system. To watch the surrounding

environment, the supervised algorithm is employed to the sensor data, and the results are compared to the fully supervised algorithm [10]. The goal of this paper is to provide a fundamental understanding of autonomous vehicles, such as which sensors are utilised, the problems of implementing autonomous vehicles, vehicle classification, and the major aims of autonomous vehicles. [14] Object detection can be accomplished in a variety of ways, including picture feature extraction, RGB value extraction, and bounding box construction [11]. The author proposes a bounding box method to identify objects based on their height, width, and colour of the object [12].

## 3. Problem Formulation

(i) Traffic coincidence is one of the predominant hassles across international-huge. Number of motorways and automobiles are growing day by day and the quantity of accidents are also growing throughout the sector.

(ii) Each year, over five million visitors are injured in the United States, according to (NHTSA) [18]. Tourism mishaps are now the second leading cause of death among young American adults. The number of road accidents resulting in death or disability rose by 3% and 2%, respectively, between 2011 and 2012.

(iii) According to (WHO), 1.25 million people worldwide die each year because of traffic injuries [19]. Traffic accidents have severe repercussions for traffic, especially on roads, at crossing, and in repainting regions, leading to increased traffic and emissions if accidents are not identified effectively and soon (Traffic Incident Management, 2013) [7].

(iv) Some of the motivating factors for vehicle detection include high computational complexity, loss of data sets, inordinate missteps start charging, detailed strength and investments of sensors on the side of lowering the mortality fee, and comprehensive power and assets of sensors on the side of lowering the mortality fee [20].

(v) All this vehicle detection and tracking systems are intended to save lives by averting road accidents using cutting-edge technology and analytics. Existing difficult conditions, such as changes in illumination, digicam fluctuation, background music, concealment, motion velocity, occlusion, and collision, result in real-time failure tracking and detection of many cars going down the street [21].

(vi) As a result, much current research has shown that detection strategies based on feature-based item identification, movement-based total detection, sensor-based detection (e.g., radar, lidar, and cameras), and so on were acquired.

(vii) Some of the measures followed by the researcher include issue check out, model multisensory trajectory, multimodal optimization functions, and lane-following multimodal prediction. Also, the effect reveals that we set a five-point threshold for the attitude difference. Then, by means of, all modes that differ from the ground path of less than 5. We can see that basic optimization allows the model to generalise effectively in both intersection and straight-road cases.

(viii) Object detection as a first stage in a visibly popular pastime and object detection using CNN are among the steps completed in this study. Sensing layer, networking layer, utility layer, and deep learning approaches are all strategies that can be applied in this study paper. The deep crash system consists of an IVI developed with car collision sensor devices, an Internet deep learning program, and a cloud-based complete control platform [22].

(ix) Typically, Internet statistics platforms transmit alarm messages and alerts based on the ultimate outcome of collision predictions, and a GPS feature for traffic coincidence is available.

(x) Some of the techniques that could be employed in this research are logistic regression, random forest, support vector machine, and comparison parameters. The techniques used include database and data sets, data set preprocessing, and proposed CNN model.

(xi) Using a transferring vehicle, we identified critical toll road segments such as street junctions, road separations, and crosswalks. Furthermore, accuracy quotes were compared among one CNN models such as Alex Net, LeNet, and VggNet, which had successful results in much research with the RoIC-CNN version, and our version's findings were matched to similar research in the literature [23].

(xii) To improve the PCD algorithm that designed the fast chronic contrastive divergence (FPCD) algorithm. Extra fast parameters were included in 2009 [13] to increase sampling speed. Desjardinsetal [14] and Cho et al. [15] introduced the parallel cooled set of rules (PT) based on sample era in 2010. In multimode goal distribution, the PT method was created to overcome the limitations of traditional sampling techniques.

(xiii) Experiments show that the PT set of regulations can produce superior techniques for RBM training while also effectively preventing any possible divergence. Several publications have been published that use deep learning method to estimate traffic flow.

(xiv) The item by MA 2017 [7] is one of the most exciting articles. This article describes at approach to assess traffic flow as photos. These pictures should then be used to expect the following kingdom of the community the use of a convolutional neural community (CNN).

*3.1. Contextualization.* Important things will be discussed here about existing RBM model.

*3.1.1. Standard RBM for Similar Scenarios.* A restricted Boltzmann machine (RBM) is a creative probabilistic artificial neural network capable of learning a probability distribution across its inputs. Restricted Boltzmann machines (RBM) have recently been shown to be powerful generative models capable of extracting useful characteristics from input records or constructing deep artificial neural networks [15]. Instead of appearing as a complete supervision version in its own right, the RBM most effectively yields an introduction for another version in such circumstances. RBMs have the potential to provide a self-contained basis for establishing competitive classifiers.

*3.1.2. Structure.* A matrices of weights $W$ of size $m * n$ is used in the standard type of RBM, which has data type (Binary search) hidden and visible units. The relationship between visual (input) unit *vi* and the hidden (output) unit *hj* is related to each weight member ($Wi$, j) of the matrix. In addition, bias weights (offsets) *ai* for *vi* and *bj* for *hj* are available. The energy of a setup (pair of Boolean vectors) ($v$, $h$) is given as given the weights and biases.

$$E(v,h) = -\sum_i a_i v_i - \sum_j b_j h_j - \sum_i \sum_j v_i w_{\mathrm{ij}} h_j. \tag{1}$$

A Hopfield network's energy function is similar to this one. The joint probability for the visible and hidden vectors is specified in terms of the energy function, as it is for General Boltzmann machines [16].

$$E(v,h) = \frac{1}{Z} e^{-E(v,h)}. \tag{2}$$

While $Z$ is a partitioning function calculated as the sum of e(− $E$ ($v$, h)) overall conceivable configuration, which can be read as a normalising constant that ensures the probabilities add up to 1. The sum of $P$ ($v$, h) over all conceivable hidden layer configurations is the marginal likelihood of a visible vector [16].

$$P(v) = \frac{1}{Z} \sum_{[11]} e^{-E(v,h)}. \tag{3}$$

Because the RBM's base graph structure is bipartite, the hidden layers signals are independent events if the visible unit inputs are present. The apparent unit activations, on the other hand, are mutually independent given the concealed unit activations. [10] That is, given a hiding unit's $h$ configuration and $m$ visible units, the likelihood value of a visible unit's $v$ arrangement is

$$P\left(\frac{v}{h}\right) = \prod_{i=1}^{m} p\left(\frac{\mathrm{vi}}{h}\right). \tag{4}$$

Conversely, the conditional probability of $h$ given $v$ is

$$P\left(\frac{h}{v}\right) = \prod_{j=1}^{n} p\left(\frac{\mathrm{hj}}{v}\right). \tag{5}$$

The individual activation probabilities are given by

$$P\left(h_j = \frac{1}{v}\right) = \sigma\left(b_j + \sum_{i=1}^{m} W_{\mathrm{ij}} v_i\right),$$
$$P\left(v_i = \frac{1}{h}\right) = \sigma\left(a_i + \sum_{j=1}^{n} W_{\mathrm{ij}} h_j\right). \tag{6}$$

The logistic sigmoid is denoted by $\sigma$. Although the hidden units of the restricted Boltzmann machine are Bernoulli, the visible units can be multinomial. The softmax function replaces the logistic sigmoid function for input nodes in this situation.

$$P\left(v_i^k = \frac{1}{h}\right) = \frac{\exp\left(a_i^k + \sum_j W_{\mathrm{ij}}^k h_j\right)}{\sum_{K=1}^{K} |\exp\left(a_i^K + \sum_j W_{\mathrm{ij}}^K h_j\right)}, \tag{7}$$

where $K$ is the number of discrete values that the visible values have. They are applied in topic modelling [7] and recommender systems [5, 24].

RBM structure and different data sets figures are given below.

In Figure 5, RBM with three visible units and four hidden units. In Figure 6, the MNIST data set. A standard written data set was used to train the RBM. It comes with 60,000 training and 10,000 test data set, as well as a greyscale image of $28 \times 28$ pixels in each sample. Figure 7: there are 19,440 training set and 24,300 testing set in this data set [27], each one is a grayscale containing $32 \times 32$ pixels. In Figure 8, the CIFAR10 data set, which includes $32 \times 32 \times 3$ pixel colour mappings. 10,000 training set, and 10,000 testing data, was generated using this data set [28]. Figures 9 and 10 are given below.

Figure 9: The CIFAR100 data set, which includes colour maps with a resolution of $32 \times 32 \times 3$ pixels. There are 10,000 training sets and 10,000 test sets in the CIFAR100 data set [28]. Figure 10shows the RBM's classification procedure.

## 4. Proposed Methodology

Proposed methodology shows that the proposed model works by passing through multiple scenarios that are given in Figure 11.

Proposed Figure 11 shows that we have taken accidental and nonaccidental images as first step of image acquisition. After image acquisition, our data set images are sent to training modified RBM where images are trained. Then next step is testing modified RBM where data set images are tested. After training and testing modified RBM stage, our data set is sent to next step that is modified RBM. Next step is generalization mechanism where our data set is passed through two parameters that are weight acceleration and coefficient adjustment. Performance is evaluated by passing our data set through multiple parameters. Last step is output of our proposed model, which shows that the resultant output is

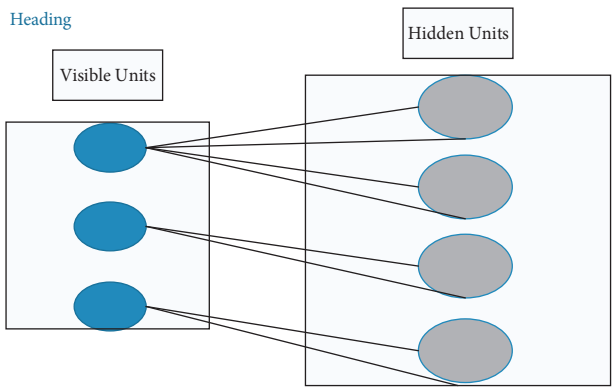


Figure 5: RBM structure.

Figure 6: The MNIST data set.

Figure 7: The MNORB data set.

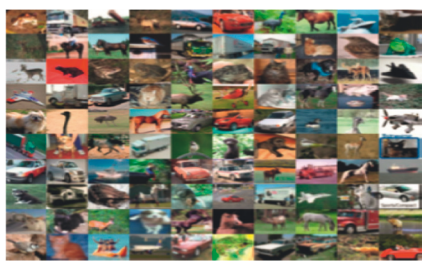

Figure 8: The CIFAR10 data set.

differentiated into two classes one is accidental images of vehicles and other is nonaccidental images of vehicles.

*4.1. Input.* First step in every model designing is input in which different accidental and nonaccidental images of vehicles on roads are taken as an input from different sources and data sets. These images act as input and after processing it will show the resultant output.

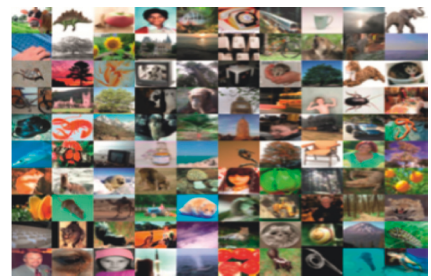

Figure 9: The CIFAR100 data set.

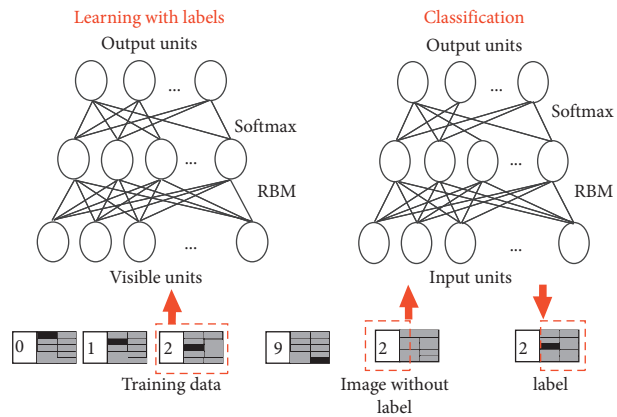


Figure 10: Classification of RBM.

*4.2. Image Acquisition.* In image processing, image acquisition can be broadly described as the operation of retrieving a picture from a source, usually a hardware-based source. The initial phase is image collecting, which entails taking a few images of both accidental and nonaccidental vehicles on toll roads and highways.

*4.3. Training-Modified RBM.* MRBM is a modelling approach that can capture the possible dissemination of information pertinent to the problem domain. It is commonly used as a building block to form more complex deep architectures, such as a deep belief network, a deep Boltzmann device, or a deep stacked automobile encoder. In fact, the RBM can be utilised as a feature representation to investigate capabilities from raw data. Furthermore, an RBM is a special type of power-based version. A modified RBM is a 2 Markov random field system that also includes a normal Markov field model. In the network, there are open and hidden gadgets that correspond to visible and hidden parameters, respectively [20]. Binary MRBM is a variant of MRBM wherein the variables in the visible and buried layers are binary. In this work, our system will present and use the binary RBM as an example. The RBM society has become a subgraph, with the majority of connections to be between public and hidden gadgets. The two types of gadgets, visible and hidden, have no connection. As a consequence of this condition, modified RBM has the following houses: the area of the visible input neurons determines the firing conditions of the neurons. The following properties of modified RBM are present: given the

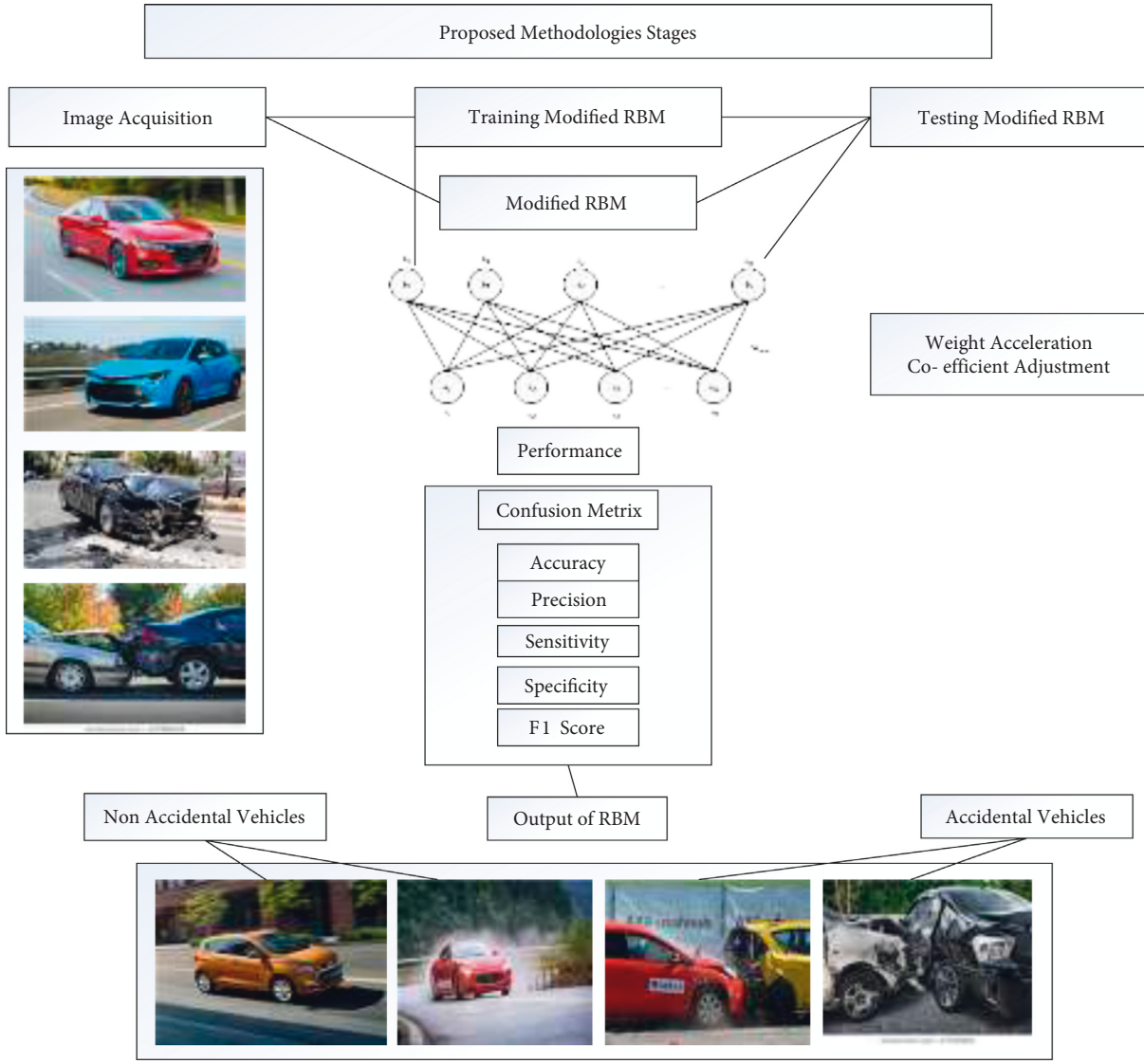


Figure 11: Proposed model.

number of visual layer neurons, the activating conditions of hidden layer neurons are independent, and conversely. Figure 1 depicts the form of an RBM. Images are sent to training adjusted RBM level after picture acquisition, where inadvertent and nonintentional allow are trained to the modified RBM.

*4.4. Testing Modified RBM.* Based on classification levels of accuracy of each technique weight replace tendencies of each set of rules, as shown in Figure 2, we explored the correlation between both the update of the MRBM society variables and the mixing start charging of the weight acceleration and coefficient adjustment sample selection chain to provide conceptual aid for improving the accuracy of the changed RBM learning set of rules. Accident and nonintentional pictures are trained and delivered to the test modified RBM level, wherein we check if the images in the learned changed RBM were effectively trained or not.

*4.5. RBM.* The RBM is a generative probabilistic neural network capable of analysing probability distributions from input data sets. RBMs can be seen in action in length reduction [8], categorization [9], content-based filtering [10], functional researching [12], subject modelling [16], radar object automatic identification [24], chip synthesizing [17], and speech repute [18]. Depending on the situation, supervised and unsupervised learning can be used to learn RBM scans. DL and RBM seem to have unique advantages for large unlabelled facts, especially in the context of massive data. Weight acceleration and coefficient adjustment are applied to the collection of train and confirmed RBM photos in a modified RBM to generalization of the collection of train and verified RBM photos.

*4.6. Performance.* Performance of modified RBM is checked or evaluated by passing through multiple parameters like Confusion Metrix, Accuracy, Precision, Sensitivity, Specifity, and F1 score.

*4.6.1. Confusion Metrix.* The confusion matrix is among the most natural and straightforward measures for determining the model's correctness and accuracy. It is used to solve classification problems where the output can be divided into two or more classes.

*4.6.2. Classification Accuracy.* In classification problems, accuracy refers to the number of accurate number of predictions across all types of predictions. It can be found using the confusion matrix or the formula below.

$$\text{Accuracy} = \left(\frac{\text{Correctly classified records}}{\text{Total Records}}\right) x100. \quad (8)$$

*4.6.3. Precision.* The precision matrix is similar to the confusion matrix, but it represents the percentage of right predictions for positive events. Being precise is what precision is all about. So, even if we just managed to capture one cancer case and correctly captured it, we are 100 percent precise.

$$\text{Precision} = \frac{\mathbf{TP}}{\mathbf{TP}} + \mathbf{TF}. \quad (9)$$

*4.6.4. Sensitivity.* The proportion of genuine positives to true positives with false negatives. Recall is not so much about correctly recording cases as it is about collecting all cases when the response is "cancer." So, if we just refer to every case as "cancer," we will have 100% recall.

$$\text{Sensitivity} = \mathbf{TN}\,\mathbf{TN} + \mathbf{FP}. \quad (10)$$

*4.6.5. Specificity.* Specificity is a metric that indicates how many patients who did not yet have cancer were classified as noncancerous by the model. Recall is the polar opposite of this.

$$\text{Specificity} = \mathbf{TN}\,\mathbf{TN} + \mathbf{FP}. \quad (11)$$

*4.6.6. F1 Score.* When we create a model to solve8 a classification problem, we do not want to have both Recall and Precision in our wallets. So, if we can get an unique score that represents both Precise (P) and Recall (R) that would be ideal (R). Precision and recall have a harmonic mean. If $x$ and $y$ are equal, the harmonic mean is a sort of average. When $x$ and $y$ are unequal; however, the smaller figure is closer to the lower number than the larger number. It can be calculated using the formula below.

$$F1\ \text{Score} = \text{Harmonic Mean}\,(\text{Precision}, \text{Recall}). \quad (12)$$

*4.7. Output of Modified RBM.* The classification accuracy of the network is a critical metric for determining the effectiveness of an RBM training process. Using the MNIST data as an experiment, the softmax classifier (Figure 12) was added to the educated RBM network's output layer, and the statistics from the RBM community's hidden layer were utilised as the inputs to teach the classifier. The top layer's output ranged from 0 to 9, with a total of 10 categories. The following technique was followed: after entering a fresh set of binary records, the appropriate binary output was obtained through the trained community parameters. The RBM's binary outputs served as the classifier's input, and they were improved in line with the RBM's outputs. The verification records were then entered into the database, and the correctness of the classification was determined. Following a review of the overall performance, a modified RBM is utilised to produce images of both accidental and non-accidental vehicles. We can see in Figure 11 that there are many types of vehicles in picture acquisition, some of which are unintentional and others of which are not. After that, the data is implemented and tested before being sent to a constrained Boltzmann machine that has been changed. The data on weight acceleration and co-efficient adjustment is examined. Then the data performance is reviewed by passing through many parameters like Confusion Metrix, Accuracy, Precision, Specificity and F1 Score. Output is generated showing accidental and non-accidental vehicles pictures as an output. As an output, photographs of both accidental and non-accidental cars are generated. A modified RBM is a random field models with a 2 network system. The network is built up of visible (samples) and invisible (variables) components, respectively [20]. The MRBM is among the most widely used basic models in deep learning. Although there are other measures for measuring the benefits of upgraded RBM learning algorithms, classification performance is the most compelling statistic that accurately reflects their benefits. Weight acceleration and co-efficient adjustment sampling techniques are the core of modified RBM training algorithms. The majority of studies on algorithmic enhancements have had trouble improving classification accuracy. In this study, the Restricted Boltzmann Machine is employed instead of the Restricted Boltzmann Machine that was used in prior papers to increase accuracy and simplicity. The following steps are included in RBM training [21]. To adjust the fast weight, the adjustment coefficient was added to the constructed weight acceleration and co-efficient adjustment in this paper. The adjustment coefficient was changed to see how it affected the entire network. MNIST was used as the sample data set in this experiment. The findings revealed that the rapid weight and adjustment coefficient included in this study could aid in the analysis of the weights. The exact value of the amount of the weight acceleration and co-efficient adjustment rose fast during the early stages of training. During the mid-late stages of training, it steadily diminished.

*Step 1.* (modelling). In modelling, the equation and the maximum - likelihood hypothesis are both utilised. RBMs are energy-based algorithms with a maximum likelihood learning goal. The power of its visible factor $v$ and hidden factor $h$ joint configurations is given by

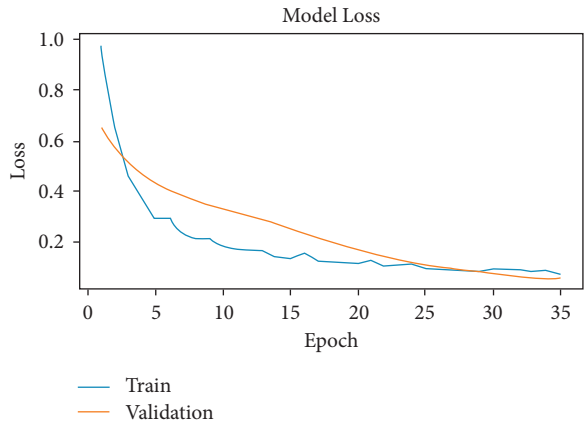


Figure 12: Training and validation loss.

$$E(v,h,\theta)E(v,h,\theta)\sum_{\mathbf{ij}}\mathbf{W}\,\mathrm{ij}\,\mathrm{vi}\,\mathrm{hj}\sum_{j}\mathrm{aj},\mathrm{hj}, \tag{13}$$

*ij* is Hidden Variable, *W*, *a*, and *b* are the parameters. The loop of *v* and *h* could be calculated as follows:

$$P\theta(v,h)\frac{1}{Z(\theta)}\exp\left(-E(v,h;\cdot\theta)\right), \tag{14}$$

$\theta$ is Parameter.

The partition function is denoted by $Z(\theta)$.

$$P\theta(v,h)\frac{1}{Z(\theta)}\exp\Big(\sum\mathrm{Di}=1\sum_{j=1}^{F}\mathbf{W}\mathrm{ij}\,\mathrm{vi}\,\mathrm{hi}+\sum_{i=1}^{D}\mathbf{v}I\,\mathrm{aj}+\sum_{j=1}^{F}\mathbf{h}\,j\,\mathrm{aj}, \tag{15}$$

$Z(\theta)$ is Partition Function.

The goal is to increase the likelihood feature P as much as possible $(v)$. The edges distribution of $P$ can be used to compute $P$ $(v)$ $(v, h)$

$$P\theta(\mathbf{v})=\frac{1}{Z(\theta)}\sum_{h}\exp\left[vT\,Wh+aTh+bTv\right], \tag{16}$$

$P\theta(\mathbf{v})$ is Likelihood Function.

*Step 2.* (estimation of parameters). For parameter estimation, the probabilistic estimate (MLE) approach is applied. To get the RBM parameters, P $(v)$ is maximised. We maximise log (P $(v)$) = $L$ () to maximise P $(v)$;

$$L(\theta)=\frac{1}{N}\sum_{n=1}^{N}\log P\theta(v(n)), \tag{17}$$

$L$ is used to obtain RBM parameters.

*Step 3.* (extremely cost-effective solution). The gradient descent approach is mostly used to find solutions with extreme values.

RBM architecture is given below in Figure 13.

It consists of four *m* and *n* denote the number of hidden neurons in the noticeable and concealed layers, in both; *v* and *h* denote the state layouts of the viewable and concealed

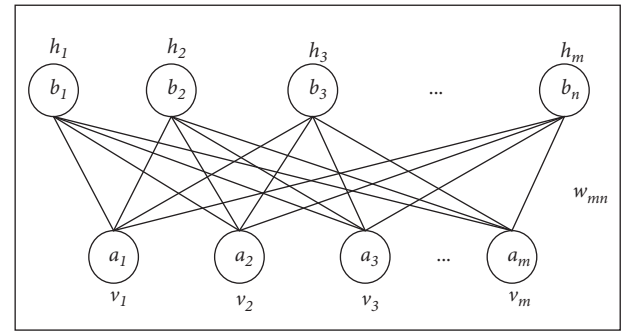


Figure 13: RBM architecture.

layers, respectively; *a* and *b* denote the bias layouts of the visible and concealed layers, respectively; and *W* denotes the weight matrix here between hidden and noticeable layers.

Using stochastic gradient descent, *L* (is first maximised. The *L* () element for *W* is then determined as follows:

$$\frac{\partial \mathrm{L}(\theta)}{\partial \mathrm{W}\,\mathbf{ij}}=\frac{1}{N}\sum_{n=1}^{N}\frac{\partial}{\partial W\,\mathbf{ij}}\log\left(\sum_{\mathbf{h}}\exp\left[v^{(n)T}\mathrm{wh}+a^{T}h+b^{T}v^{(n)}\right]\right)$$

$$-\frac{\partial}{\partial W\,\mathbf{ij}}\log Z(\theta). \tag{18}$$

$$=E_{p\,\mathrm{data}}\left[v_i\mathbf{h}_j\right]-E_{p\theta}\left[v_i\mathbf{h}_j\right]. \tag{19}$$

$\partial W$ is RBM Parameters, $P_\theta$ is Samples satisfying the distribution.

The first half of the equation is simple to compute. The average *vi* and hj values across all data sets are determined. However, because of the computational complexity, the second half of the equation, which involves all $2|v|+|h|$ configurations of *v* and *h*, is difficult to solve.

The formula's second half is equivalent to

$$\sum_{\mathrm{Vih}}\mathbf{vi}\mathbf{h}\,jP_{\theta}(v,\mathbf{h}). \tag{20}$$

Because the gradient's analytical solution cannot be determined, present training algorithms rely heavily on the sampling. To generate the samples that satisfy the distribution, a Markov chain with a density function $P(v)$ is first constructed. Monte Carlo simulations are then used to approximate the gradient:

$$\Delta a_i=v_i^{(0)}\text{-}v_i^{(k)}. \tag{21}$$

According to the previous study, the classical approach can be improved by increasing weight acceleration and co-efficient adjustment. Despite a 2% increase in classification accuracy and a large improvement in the mix rate of the new algorithm's weight acceleration and co-efficient adjustment chain, the probability of the enhanced PCD method's transference operators was only 0.94. As a result, by altering the weight update based on the typical CD method, the goal was to improve the mix rate of the weight acceleration and co-efficient adjustment. The weight increase must meet the two standards listed below.

(1) The changing of weights should be done fast at first. A sudden increase in the weight training at the start is useful for increasing the randomness of the transmission operator, leads to a rapid increase in the weight acceleration and co-efficient adjustment mixing rate, as according Corollary 2 of the weight acceleration and co-efficient adjustment convergence theorem.

(2) The weight updates should show a decreasing range in the middle and end of the training cycle. As the weight grows, the required $X$ period of the transfer operators will increase. According to Corollary 1 derived from the centralization principle of weight acceleration and co-efficient adjustment, when the transmission likelihood of the transmission controller is 1, the flexible domain of the transmission operator constantly reduces if the accurate amount of the weight increases upon sampling. As a result, the mixing rate for weight acceleration and co-efficient adjustment slows. As a consequence, if the overall number of the weight drops after the transition probability of the transfer operator reaches 1, the weighting of the transfer operator will expand its inability domain. This will enhance the weight acceleration and co-efficient adjustment mixing rate, consequently increase the model performance [25].

This paper provides an accelerated weight fast $W$ and adjustment coefficient, as well as a weight acceleration and coefficient adjustment algorithm. The traditional weights are adjusted in the same way as the accelerating weights presented in this paper. In the accelerated weight update, the gap between both the data and modelling predictions is also a factor. The overall weight of the overall infrastructure, on either hand, is the sum of the accelerating and standard weights, ensuring that weight updates happen promptly during the early phases of learning. The adjustment coefficient in this study has the ability to vary the accelerated weight update rate. The adjustment coefficient can be modified from 0 to 1, effectively slowing down the tendency of rapid weight updates during the middle and finish of training. By attempting to start introducing the accelerated weight and adjustment coefficient, the suggested weight acceleration and coefficient adjustment technique can improve the transfer function of the transmission operators and the smoothing rate of a weight acceleration and coefficient adjustment chains, thus working to improve the algorithm's classification accuracy. The formula that was utilised to adjust the weight is as follows:

The data input $v$ is selected to generate the hidden layer data, similar to the classic RBM training procedure. The input data are represented by $v^+ = v$ in this case.

$$h^+ = P\left(\frac{h}{v^+}+, W\right), \tag{22}$$

$h/v^+$ is the input data

$$\mathbf{h}^- = \mathbf{P}\left(\frac{\mathbf{h}}{\mathbf{v}^+}+, \mathbf{W} + \text{fast}\,\mathbf{W}\right). \tag{23}$$

The positive and negative gradients are updated after the hidden layer information is calculated.

$$\begin{aligned}\mathbf{W}^+ &= \mathbf{v}^{+T}\mathbf{h}^+,\\ \mathbf{W}^- &= \mathbf{v}^{-T}\mathbf{h}^-.\end{aligned} \tag{24}$$

After that the hidden layer data can be used to calculate the new input layer data. The weights are equal parts traditional and accelerated:

$$v^- = h^- = p\left(\frac{v^-}{h}W + \text{fast}\,W\right). \tag{25}$$

$h^-$ is the accelerated weight.

The weight update gradient is divided into two sections: standard weight update and rapid weight update:

$$\Delta W = W^+ + W. \tag{26}$$

$W^+$ is traditional weight update and accelerated weight update.

The formulae described below govern both traditional and expedited weight updates. The adjustment coefficient is used to regulate the rapid weight update in this paper, and it can also be used to control the trend change

$$W = W + \Delta W. \tag{27}$$

$$\text{fast}\,W = \boldsymbol{\xi} * \text{fast}\,\mathbf{W} + \boldsymbol{\Delta}\mathbf{W}. \tag{28}$$

fast W is Adjustment Co-efficient.

## 5. Experimental Setup

All the experiments that are done related to accident detetction in autonomous vehicles using modified restricted Boltzmann machine are briefly discussed in this section.

*5.1. System Description.* System that we use for simulation purpose is corei5 4th generation with 16 GB Ram and 512 GB SSD. The tools that are used for simulation purpose are anaconda and python 3.9. The library that we used is Tansorflow, Keras for Neural network.

*5.2. Data Set Description.* The data sets consist of total 1000 vehicles images in which 500 are accidental images of vehicles and 500 are nonaccidental images of vehicles that are taken from kaggle, and size of each image is $150 \times 150$. In first 4 images, the first two images show are nonaccidental images of vehicles and the other two show the accidental images of vehicles.

*5.3. Data Set Division.* The data set is divided into different train and test ratio, which are as follows:

(i) 70% train and 30% test

(ii) 60% train and 40% test

(iii) 50% train and 50% test

*5.4. Parameter Tuning.* Following are the parameter tuning that is set for proposed model is discussed in this section.

*5.5. Parameter Tuning in Modified Restricted Boltzmann Machine Model.* Different parameters and their values are used in this Table 1, for modelling the MRBM model. All the parameters and values are set to maximise the model performance. These parameters and values are used to increase the model performance. Batch size is 64, and epoch's size is set at 35, 40, and 50. Parameter tuning in MRBM for all experiments is given below.

## 6. Results and Discussion

The results of our proposed models are as discussed in this section.

*6.1. Modified Restricted Boltzmann Machine Model.* The results of all data set division based on CNN mode is given as below:

*Experiment 1.* The Modified RBM Model has been trained on 70% of the data chosen at random, and the remaining 30% is used to evaluate the model. Our accuracy was 98%, which was higher than typical RBM. The performance of the Modified RBM Model was also compared to that of three other common ML techniques: ANNs, SVMs, and RBMs, with the findings published in Supplementary Materials. The Modified RBM Model outperformed the other two approaches.

Figure 14 is given below here.

As illustrated in Figure 14, the accuracy we achieved is 98% which is greater than standard RBM. So we can see in this report that Modified RBM Model performed best. Figure 15 is given below.

As illustrated in this Figure 15 which shows that 35 Epoch are used for training and validation purpose. The upper sky blue line shows the train data while the lower orange line shows the validation data. The MRBM model have 0.21 training accuracy and 0.72 validation accuracy at start to the end point of training accuracy of model which is 97% and validation accuracy of MRBM model is 98%. Figure 12 is given below.

As illustrated in Figure 12 which shows that 35 Epoch are used for training and validation purpose. The lower sky blue line shows the train data while the upper orange line shows the validation data. At start, our model give training loss of 0.85 and a validation loss of 0.65. But when epoch size increases time by time, the results become more better and better and at last the model gives training loss of 0.11 and a validation loss of 0.12. The $X$-axis represents the epoch count, and the $Y$-axis represents the testing and validation loss. The loss value varies depending on the learning rate. If the learning rate is low, the loss value decreases gradually. If the learning rate is high, the loss value decreases rapidly. Figure 16 is given below.

Table 1: Parameter tuning in MRBM for all experiments.

| Parameter | Values |
|---|---|
| Layers | 2 |
| Optimization function | Adam |
| Activation function | Relu and softmax |
| Learning rate | 0.0001 |
| Epoch size | 35,40,50 |
| Batch size | 64 |
| Loss function | Categorical crossentropy |

| | precision | recall | f1-score | support |
|---|---|---|---|---|
| 0 | 0.99 | 0.98 | 0.99 | 115 |
| 1 | 0.96 | 0.98 | 0.97 | 56 |
| accuracy | | | 0.98 | 171 |
| macro avg | 0.98 | 0.98 | 0.98 | 171 |
| weighted avg | 0.98 | 0.98 | 0.98 | 171 |

Figure 14: Report.

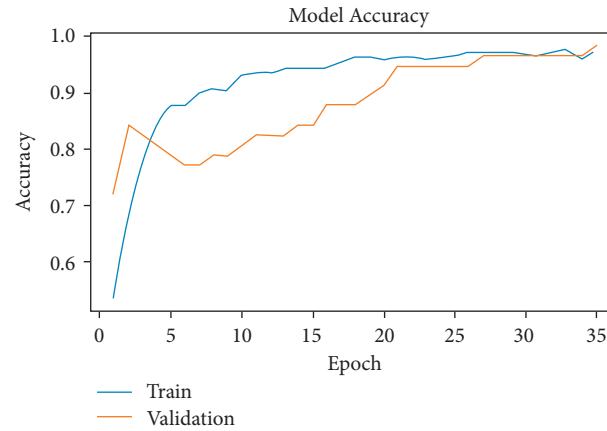


Figure 15: Testing and validation accuracy.

In ROC, Figure 16 FPR and TPR limit is set to 1 in this paper. Using knn ($n$-neighbors = 3), ROC curve is achieving maximum value for data set images. Figure 17 is given below.

As shown in Figure 17, the confusion matrix chart, where the column represents instances in a class label and the row represents examples in the actual class. Correct prediction is shown by values on the matrices diagonal, whereas wrong prediction is indicated by values outside of the matrix diagonal. The value boxes 42 and 101 are accurately predicted, whereas 56 and 0 are wrongly projected. Our technology correctly predicts and detects nonaccidental and accidental vehicles 96% of the time. Figure 18 is given below.

Here we can see in Figure 18 of test pseudocode that the accuracy we obtained in it is 96%.

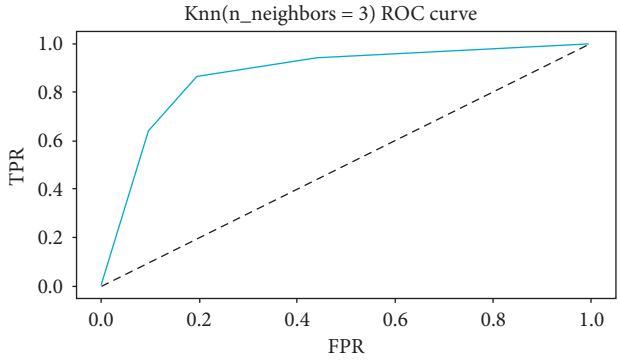


Figure 16: Receiver operating characteristic.

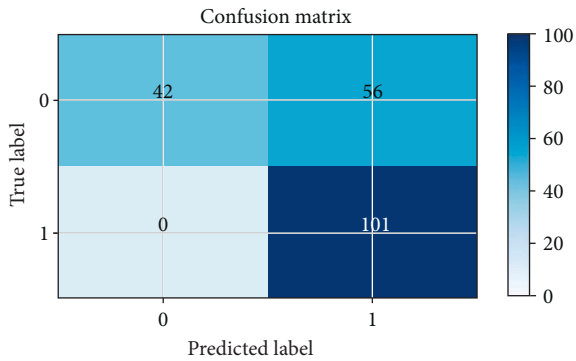


Figure 17: Confusion Matrix_Ctscan.

```
output_test = model.predict (x_test)
print ("test auc:", roc_auc_score (y_test, output_test))

test auc: 0.9641341685188927
```

Figure 18: Test pseudo code.

Performance attributes' values for experiment # 1 table is given below here in Table 2.

*Experiment 2.* In the Experiment 2, the accidental and nonaccidental vehicles data set was divided into the 60% and 40% ratio for the training and the testing in which it executed better and achieved 96% accuracy. Figure 19 is given below here.

As shown in Figure 19 which shows that by using 60% of images data sample is used randomly and 40% of data is used as training data. The accuracy achieved from this type of data is 96% which is high from existing work. Figure 20 is given here below.

As shown in Figure 20 which shows that the training accuracy of MRBM model is 96% and the validation accuracy of model is 94.5%. The 40 Epochs count is shown in *X*-axis, and the training and validation accuracy are shown in *Y*-axis. The red line shows training accuracy and the dark blue line shows validation accuracy. As when we began our model on running it give the 0.30% training and 0.84% validation accuracy; however, when Epochs size increment time by time the outcomes becomes better and finally MRBM model give 96% training and 94.5% validation accuracy. Figure 21 is given here below.

The training loss of the MRBM model is 0.15, and the validation loss is 0.19, as shown in Figure 21. The epoch count is represented by the X-pivot, while the verification and validation loss is represented by the Y-pivot. Depending on the learning rate, the loss value fluctuates. The loss value decreases considerably if the training rate is low. The loss value drops quickly if the training error is large. Finally, the training error is 96% and the validation error is 50%. Figure 22 is given here below.

As shown in Figure 22 that shows the confusion matrix predicted label chart where dark blue box values are correct and white box values are incorrect, and we have achieved 92% accuracy from 60 40 data partition. Figure 23 is given here below.

As shown in Figure 23, receiver operating characteristic that shows false-positive rate set value is 1.0 and true positive set value is also 1.0. The red line shows AUC obtaining high accuracy of value 0.96 of range 1.0. Figure 24 is given here below.

As shown in Figure 24 that shows the sensitivity and specifity value which is 1.00 and 0.80. These values are obtained from 60 40 data partition. Performance attributes values for experiment # 2 are given below here in Table 3.

*Experiment 3.* In Experiment 3, the accidental and nonaccidental vehicles data set was divided into the 50% and 50% ratio for the training and the testing purpose in which it executed better and achieved 98% accuracy. Figure 25 is given below.

As illustrated in Figure 25 that shows that by using 50% of images data sample is used randomly and 50% of data is used as training data. The accuracy achieved from this type of data is 98%. Figure 26 is given below.

As illustrated in Figure 26 that shows that the 50 Epochs count is shown in *X*-axis, the training and validation accuracy are shown in *Y*-axis. The light blue line shows training accuracy and the light orange line shows validation accuracy. When we began our model on running, it gives the 0.67% training and 0.69% validation accuracy. However, when Epochs size increment time by time the output becomes better and finally MRBM model give 80% training and 78.5% validation accuracy. Figure 27 is given below.

As illustrated in Figure 27 that shows that the X-pivot represents the epoch count, and the Y-pivot represents the testing and validation loss. The loss value changes relying upon the learning rate. When we began our model, loss training and validation loss testing at stat training loss value was 1.0, and the validation loss was 0.93. At last, the training loss is 0.2, and validation loss is 0.62. Figure 28 is given below.

As illustrated in Figure 28,receiver operating characteristic that shows false-positive rate set value is 1.0 and true-

Table 2: Performance attributes values for experiment # 1.

| Model | Data division | Training accuracy (%) | Testing accuracy (%) | Sensitivity | Specificity | Precision | | Recall | | F1 score | |
|---|---|---|---|---|---|---|---|---|---|---|---|
| | | | | | | A | N | A | N | A | N |
| MRBM | 70% and 30% | 97 | 98 | 0.96 | 1 | 0.96 | 0.99 | 0.98 | 0.98 | 0.97 | 0.99 |

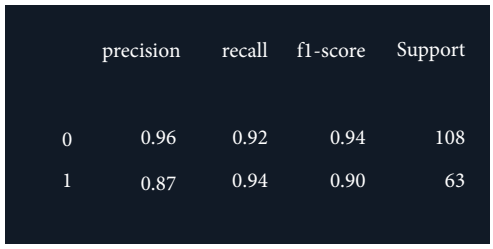


Figure 19: Report.

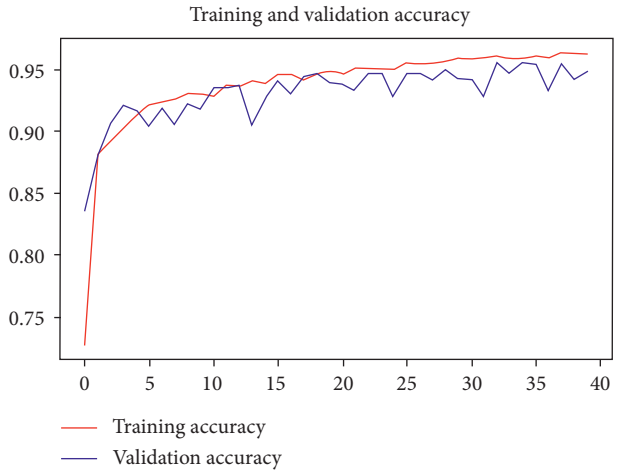


Figure 20: Training and validation accuracy.

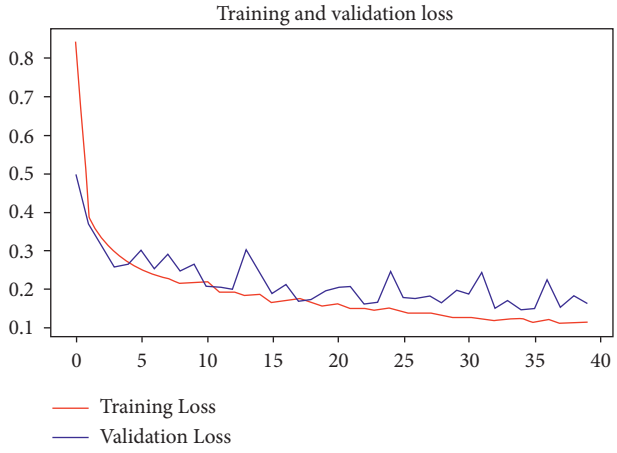


Figure 21: Training and validation loss.

positive set value is also 1.0. The red line shows AUC obtaining high accuracy of value 0.98 of range 1.0. Figure 29 is given below.

As illustrated in Figure 29 that shows the confusion matrix predicted label chart where blue box data values are

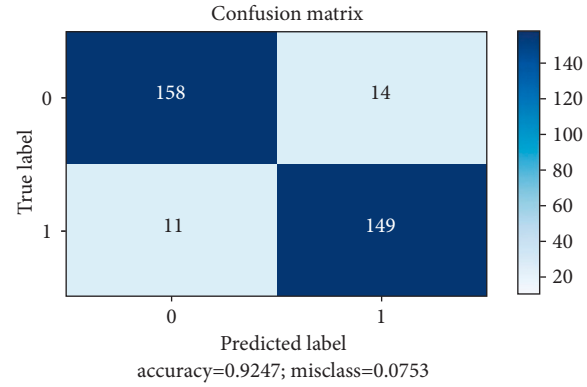


Figure 22: Confusion matrix.

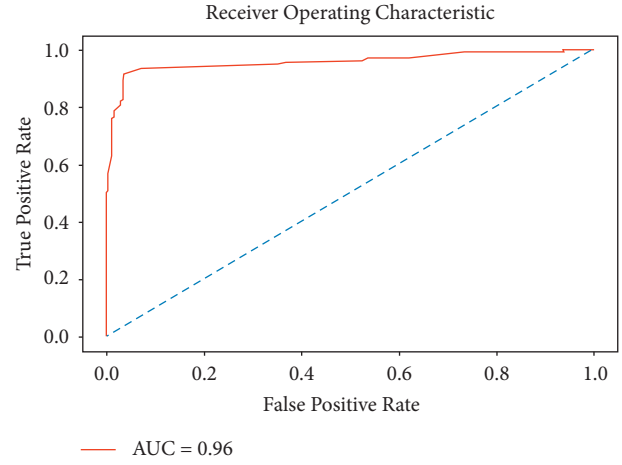


Figure 23: Receiver operating characteristic.

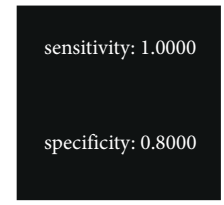


Figure 24: ACC report.

correct and other white box are incorrect, and we have achieved 98% accuracy from 50 50 data partition. Performance attributes' values for experiment # 3 are given here in Table 4.

*6.2. Comparison.* Artificial Neural Network, Support Vector Machine, and Restricted Boltzmann Machine techniques are compared with our proposed work. Comparison with other techniques are given below in Figure 30.

Table 3: Performance attributes values.

| Model | Data division | Training accuracy (%) | Testing accuracy (%) | Sensitivity | Specificity | Precision | | Recall | | F1 score | |
|---|---|---|---|---|---|---|---|---|---|---|---|
| | | | | | | A | N | A | N | A | N |
| MRBM | 60% and 40% | 96 | 94.5 | 1 | 1 | 0.87 | 0.96 | 0.94 | 0.92 | 0.90 | 0.94 |

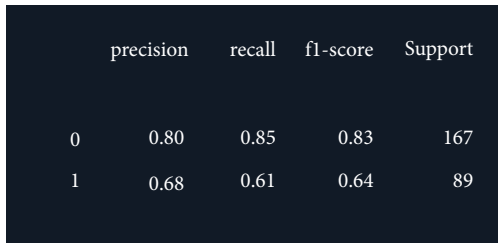


Figure 25: Report.

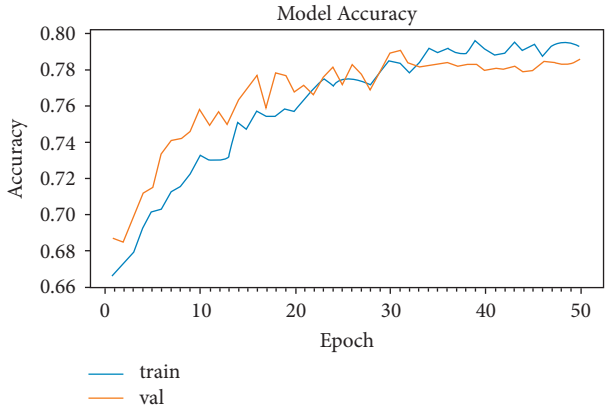


Figure 26: Testing and validation accuracy.

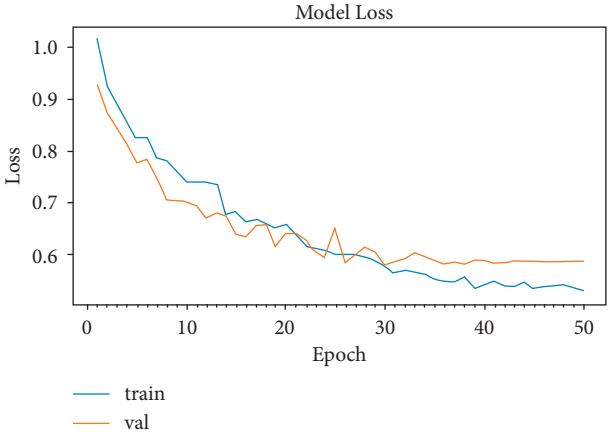


Figure 27: Training and validation loss.

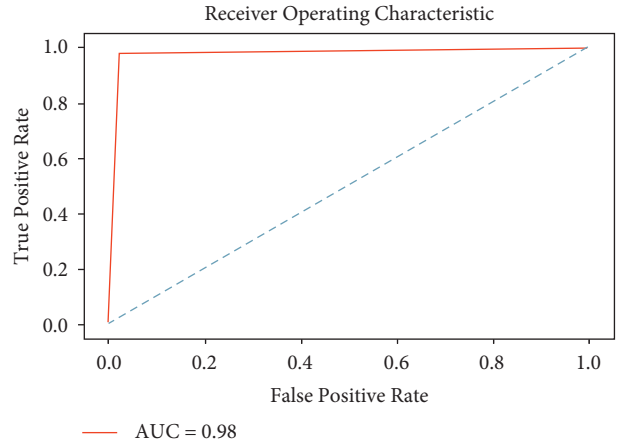


Figure 28: Receiver operating characteristic.

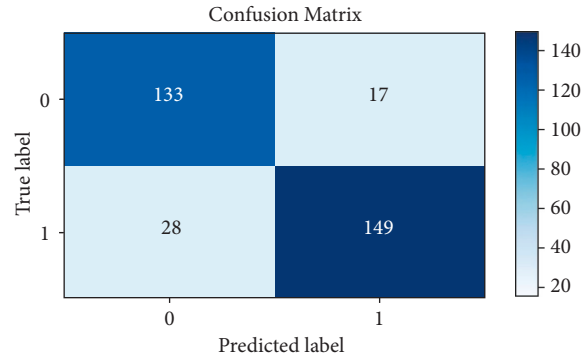


Figure 29: Confusion Matrix_Ctscan.

Our model offers a method for extracting both accidental and nonaccidental vehicles detection from MRBM model using a structured feature selection procedure. Our model demonstrates that the deep learning method is effective in classifying accident detection in vehicles. Deep learning surpasses traditional accident detection methods, according to the findings. We have in comparison our proposed model with other's data, and the chart is given in Figure 31 [17].

To compare the achieved results from Experiment 1 (70%:30% data set division ratio), we employ statistical metrics: accuracy and precision, etc. For accidental vehicles and nonaccidental vehicles images with other models. Figure 32 is given below here.

To evaluate the achieved results from Experiment 2 (60%:40% data set division ratio), we employ our result on statistical metrics: accuracy and precision etc. For accidental vehicles and non-accidental vehicles images with other models. Figure 33 is given below here.

To check and compare the achieved results from Experiment 3 (50%:50% data set division ratio), we employ our result on statistical metrics: accuracy and precision, etc. For accidental vehicles and nonaccidental vehicles images with other models. Figure 34 is given below here.

Table 4: Performance attributes values.

| Model | Data division | Training accuracy (%) | Testing accuracy (%) | Sensitivity | Specificity | Precision | | Recall | | F1 score | |
|---|---|---|---|---|---|---|---|---|---|---|---|
| | | | | | | A | N | A | N | A | N |
| MRBM | 50% and 50% | 80 | 78.5 | 1 | 1 | 0.68 | 0.80 | 0.61 | 0.85 | 0.64 | 0.83 |

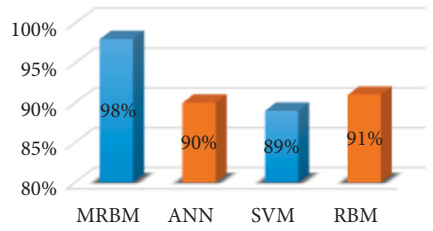


Figure 30: Comparison with other techniques.

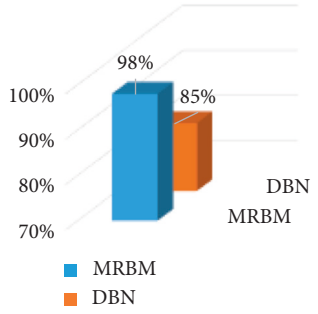


Figure 31: Comparison with other models.

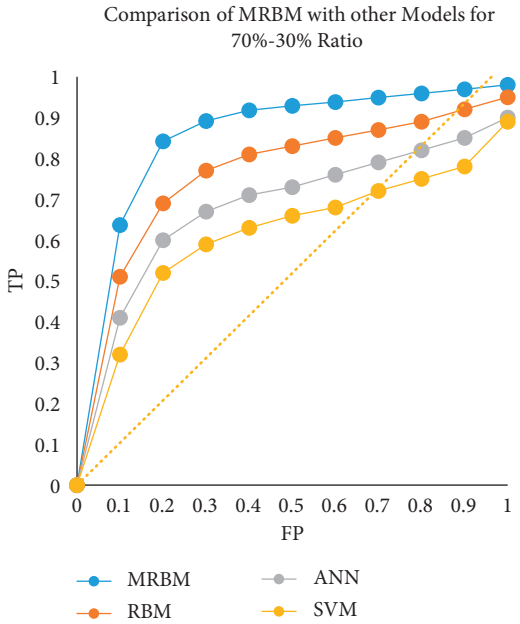


Figure 32: Comparison of MRBM performance with other models for Experiment 1 (70%:30% data set division ratio).

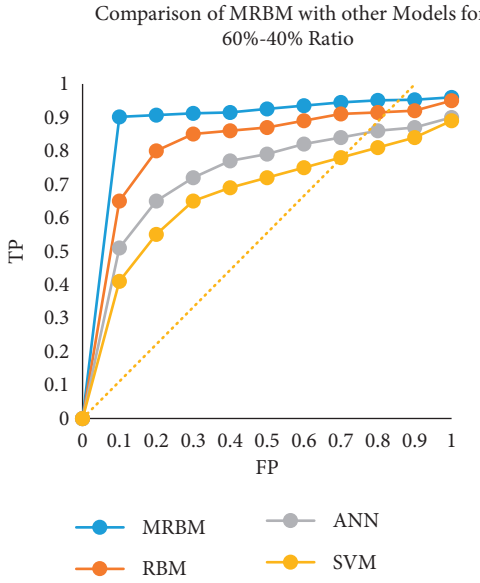


Figure 33: Comparison of MRBM performance with other models for Experiment 2 (60%:40% data set division ratio).

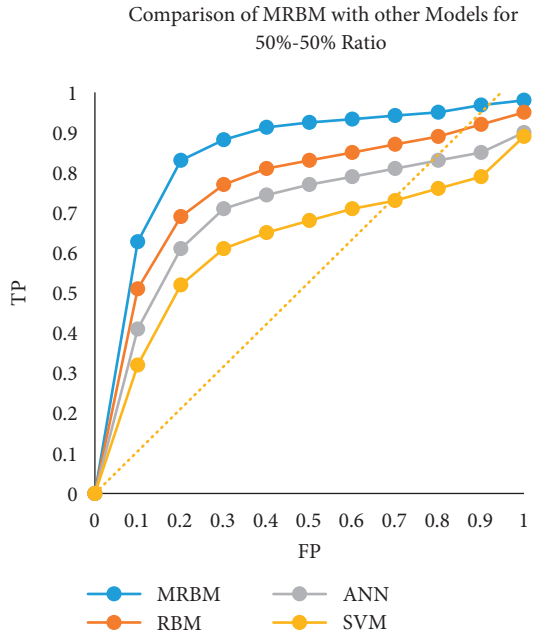


Figure 34: Comparison of MRBM performance with other models for Experiment 3 (50%:50% data set division ratio).

## 7. Conclusion

The goal of this work was to provide an analysis on accelerated weights and the adjustment coefficient parameter to increase the accuracy of classification of the MRBM training algorithm. We are following overfitting and underfitting issues, and modified RBM was used instead of conventional RBM. Multiple types of accidents have been identified in a variety of vehicles. Overfitting is a problem with standard RBM, thus we used MRBM to overcome it. For classical algorithms, experimental investigation demonstrated that the mixed ratio of accelerated weights and the adjustment coefficient can be increased. The accelerated weights and adjustment coefficient were used in this work to improve the training weights update. In addition, the proposed method hm increased MRBM accuracy and reduced training time. The new MRBM algorithm outperformed the standard RBM training technique in terms of classification accuracy. Proper control trials were generated in this research using experiment data sets (accidental and nonaccidental vehicles images), and the results were evaluated using the MRBM mixing ratio, sampling comparison, classification accuracy, training time, and two parameters. The suggested MRBM algorithm demonstrated strong sampling convergence properties, according to the experimental results. MRBM can minimise training time and improve classification accuracy over traditional methods. Also, based on the results of the experiments, it is possible to conclude that the suggested MRBM algorithm is universal. To evaluate the model, the Modified RBM Model was trained on data picked at random. Our accuracy was 98%, which was greater than the traditional RBM. The Modified RBM Model performance was compared to three other common machine learning techniques: ANNs, SVMs, and RBMs.

## 8. Future Work

Testing the data sets on other deep learning models to see what their output will be in future. Model testing on other data sets to see their generated results. If we increase our data set image size, then it may affect our model's performance. Future work will focus on upgrading the training model and increasing the number of samples used to train the model, which may increase the accuracy.

## Data Availability

The data collected during the data collection phase are available from the corresponding authors upon request.

## Disclosure

The authors confirm that the paper results are not clinical results based on clinical trials, instead they are a computer-based study, in which they have trained a machine learning model using Images. Therefore, there is no need of a trial registration number.

## Conflicts of Interest

No potential conflicts of interest have been declared by the authors.

## Acknowledgments

This work was supported by the Qatar National Library, Doha, Qatar, and in part by the QU Internal Grant Qatar University Internal under Grant IRCC-2021-010.

## References

[1] L. Wu, Z. Jiang, W. Cheng, X. Zuo, D. Lv, and Y. Yao, "Major accident analysis and prevention of coal mines in China from the year of 1949 to 2009," *Mining Science and Technology*, vol. 21, no. 5, pp. 693–699, 2011.

[2] M. Fogue, P. Garrido, F. J. Martinez, J. Cano, C. T. Calafate, and P. Manzoni, "Automatic accident detection: assistance through communication technologies and vehicles," *IEEE Vehicular Technology Magazine*, vol. 7, no. 3, pp. 90–100, 2012.

[3] M. Hnewa and H. Radha, "Object detection under rainy conditions for autonomous vehicles: a review of state-of-the-art and emerging techniques," *IEEE Signal Processing Magazine*, vol. 38, no. 1, pp. 53–67, 2021.

[4] K. S. Baker, *Traffic Collision Investigation*, Northwestern University Center for Public Safety, Evanston, IL, U.S.A, 2001.

[5] G. Grayson, "Company cars and road safety," in *BEHAVIOURAL RESEARCH IN ROAD SAFETY IX. PA3524/99*, pp. 65–70, Transport Research Laboratory, Crowthorne, U.K, 1999.

[6] H. Cui, V. Radosavljevic, F. C. Chou et al., "Multimodal trajectory predictions for autonomous driving using deep convolutional networks," in *Proceedings of the 2019 International Conference on Robotics and Automation (ICRA)*, 20 May 2019.

[7] W. J. Chang, L. B. Chen, and K. Y. Su, "DeepCrash: a deep learning-based internet of vehicles system for head-on and single-vehicle accident detection with emergency notification," *IEEE Access*, vol. 7, pp. 148163–148175, 2019.

[8] N. Dogru and A. Subasi, "Traffic accident detection using random forest classifier," in *Proceedings of the 2018 15th learning and technology conference (L&T)*, IEEE, Jeddah, Saudi Arabia, 25 February 2018.

[9] A. Misra, *Detection of Driver Cognitive Distraction Using Machine Learning Methods*, University of Waterloo Library 200 University Avenue West Waterloo, Ontario, Canada, 2020.

[10] L. Li, Y. Lin, B. Du, F. Yang, and B. Ran, "Real-time traffic incident detection based on a hybrid deep learning model," *Transportmetrica: Transportation Science*, vol. 18, no. 1, pp. 78–98, 2020.

[11] U. Alvi, M. A. K. Khattak, B. Shabir, A. W. Malik, and S. R. Muhammad, "A Comprehensive study on IoT based accident detection systems for smart vehicles," *IEEE Access*, vol. 8, pp. 122480–122497, 2020.

[12] V. Tümen and B. Ergen, "Intersections and crosswalk detection using deep learning and image processing techniques," *Physica A: Statistical Mechanics and its Applications*, vol. 543, Article ID 123510, 2020.

[13] H. Khayyam, B. Javadi, M. Jalili, and R. N. Jazar, "Artificial intelligence and internet of Things for autonomous vehicles," in *Nonlinear Approaches in Engineering Applications*, pp. 39–68, Springer, Cham, Berlin, Germany, 2020.

[14] A. B. Parsa, A. Movahedi, H. Taghipour, S. Derrible, and A. Mohammadian, "Toward safer Highways, application of XGBoost and SHAP for real-time accident detection and Feature analysis," *Accident Analysis & Prevention*, vol. 136, Article ID 105405, 2020.

[15] H. Larochelle, M. Mandel, R. Pascanu, and Y. Bengio, "Learning algorithms for the classification restricted Boltzmann machine," *Journal of Machine Learning Research*, vol. 13, no. 1, pp. 643–669, 2012.

[16] J. Chung and H. J. Kim, "An automobile environment detection system based on deep neural network and its implementation using IoT-enabled in-vehicle air quality sensors," *Sustainability*, vol. 12, no. 6, pp. 2475–2020, 2020.

[17] B. P. Saha and J. K. Rout, "Analysis and prevention of road accidents," *Lecture Notes in Electrical Engineering*, vol. 709, pp. 107–118, 2021.

[18] M. Haris and A. Glowacz, "Road object detection: a comparative study of deep learning-based algorithms," *Electronics*, vol. 10, no. 16, p. 1932, 2021.

[19] Z. Zhang and Q. J. M. He, "A deep learning approach for detecting traffic accidents from social media data," *Transportation Research Part C: Emerging Technologies*, vol. 86, pp. 580–596, 2018.

[20] S. Ali, M. Adeel, S. Johar, M. Zeeshan, S. Baseer, and A. Irshad, "Classification and prediction of software incidents using machine learning techniques," *Security and Communication Networks*, vol. 2021, pp. 1–16, 2021.

[21] D. Sudha and J. Priyadarshini, "An intelligent multiple vehicle detection and tracking using modified vibe algorithm and deep learning algorithm," *Soft Computing*, vol. 24, no. 22, pp. 17417–17429, 2020.

[22] Z. Yang, S. Ali, W. Ding, I. A. Abbasi, and M. F. Khan, "A Way to automatically generate lane level traffic Data from Video in the intersections," *Journal of Advanced Transportation*, vol. 2021, pp. 1–10, 2021.

[23] A. R. Pathak, M. Pandey, and S. Rautaray, "Application of deep learning for object detection," *Procedia Computer Science*, vol. 132, pp. 1706–1717, 2018.

[24] R. Padilla, S. L. Netto, and E. A. da Silva, "A survey on performance metrics for object-detection algorithms," in *Proceedings of the 2020 International Conference on Systems, Signals and Image Processing (IWSSIP)*, 1 July 2020.

[25] Q. Wang, X. Gao, and K. Wan, F. Li and Z. Hu, A novel restricted Boltzmann machine training algorithm with fast Gibbs sampling policy," *Mathematical Problems in Engineering*, vol. 2020, pp. 1–19, Article ID 4206457, 2020.

[26] Z. Yang, S. Ali, W. Ding, I. A. Abbasi, and M. F. Khan, "A way to automatically generate lane level traffic data from video in the intersections," *Journal of Advanced Transportation*, vol. 2021, Article ID 4764174, 10 pages, 2021.

[27] Y. Lecun, F. S. Huang, and L. Bottou, "Learning methods for generic object recognition with invariance to pose and lighting," in *Proceedings of the 2004 IEEE Computer Society Conference on Computer Vision & Pattern Recognition*, Washington, DC, USA, June 2004.

[28] J. Schmidhuber, *New Millennium AI and the Convergence of History: Update of 2012*, The Frontiers Collection, Springer, Berlin, Germany, 2012.